MJFAS
Malaysian Journal of Fundamental and Applied Sciences

Batur *et al.* | Malaysian Journal of Fundamental and Applied Sciences, Vol. 20 (2024) 923–938

RESEARCH ARTICLE

Recommendations for Protective Actions Based on Projected Public Health Risks Following a Postulated Nuclear Power Plant Accident

Maryna Batur[a]*, Reha Metin Alkan[b], Himmet Karaman[b], Haluk Ozener[c]

[a]Graduate School, Istanbul Technical University, 34469, Istanbul, Turkiye; [b]Department of Geomatics Engineering, Istanbul Technical University, 34469, Istanbul, Turkiye; [c]Department of Geodesy, Kandilli Observatory and Earthquake Research Institute, Bogazici University, 34684, Istanbul, Turkiye

Abstract This study conducted a regional assessment of the environmental and health consequences due to the release of radionuclides, including the most harmful, such as Cs-137 and I-131, from a hypothetical reactor accident at the first Nuclear Power Plant (NPP), Akkuyu Nuclear Power Plant, in Turkiye under different meteorological conditions. Simulations of the atmospheric flow were done using a Gaussian-based probabilistic model. Based on the estimated air and land contamination, radiation doses and cancer risks to the population were calculated. The assessment results were then compared with the criteria for protective actions in the event of a radioactive release and were subsequently used to assess the sufficiency of the Precautionary Action Zone (PAZ) and Urgent Protective Zone (UPZ) provided by regulations. The assessment indicated that evacuation outside the UPZ would likely be required during the early phase of the emergency, while sheltering indoors might be necessary up to 80 km. Protective actions such as restrictions on being outdoors or iodine prophylaxis are needed far beyond the radius of the UPZ. These results provide important insights into safe protective measures to reduce the risk of radiation-related cancer when considering a hypothetical severe nuclear accident. In addition, the results of this study aim to improve the current nuclear emergency response program and support nuclear decision-making.

Keywords: Hypothetical accident, gaussian plume, nuclear hazard mapping, emergency response, protective actions.

Introduction

A massive release of radiation at a damaged Nuclear Power Plant (NPP) can pose a significant threat to the population and cause further environmental and socio-economic consequences [1]. The primary concern in accident-affected areas is the risk of radiation exposure and the subsequent risk of developing cancer [2]. As many studies show, after the Chernobyl accident, thousands of people, including children, within a radius of hundreds of kilometers, developed incurable diseases such as thyroid cancer [3]. Hovewer, after Fukushima, the cancer doses were much lower compared to Chernobyl, mainly due to more efficient and better-implemented response coordination [4-5]. Nevertheless, past disasters such as Chernobyl and Fukushima have clearly proven the relevance of nuclear emergency preparedness. According to the International Atomic Energy Agency (IAEA), a nuclear emergency is divided into three main steps: (1) preparedness, which involves a continuous cycle of planning, training, and educational programs; (2) the emergency exposure situation; and (3) disaster recovery, a long-term phase aimed at restoring living conditions in affected areas [6]. The emergency exposure situation begins with the announcement of a radiation emergency and consists of immediate and early phases. The immediate phase first involves identifying conditions that may require the application of protective actions to the public before those actions can be taken. The early response phase starts when radiological conditions are clear enough for protective measures, such as evacuation, sheltering, and/or iodine distribution, to be implemented. To support the predetermined strategy of these protective measures, so-called

***For correspondence:**
baturm20@itu.edu.tr

Received: 07 May 2024
Accepted: 31 July 2024

Emergency Planning Zones (EPZs) are established around NPPs in each country in line with international and national emergency plans. Local agencies then implement specific actions to reduce adverse health effects. EPZs include the Precautionary Action Zone (PAZ), Urgent Protective Zone (UPZ), Extended Planning Zone (EPZ), and Ingestion and Commodities Planning Distance (ICPD) zone, with radii of 3-5 km, 30 km, 100 km, and 300 km, respectively [7]. Depending on the course of the accident, protective measures within the PAZ must be executed once radioactive materials have been released into the atmosphere. In contrast, protective measures within the UPZ can be implemented based on the results of continuous environmental monitoring. However, protective measures must be clearly defined in advance in all cases. Although the size of EPZs has been predefined by the IAEA, they may vary depending on the type of release, the spatiotemporal distribution of radionuclides in the atmosphere, and their subsequent deposition on the ground, which, in turn, change with meteorological conditions. Moreover, the population is exposed to radiation through inhalation and deposition of radionuclides [8]. Thus, a successful emergency response requires not only the rapid implementation of predetermined protective measures but also an appropriate assessment of atmospheric dispersion, ground deposition patterns, and a careful estimation of the Total Effective Dose Equivalent (TEDE), thyroid doses, and likely cancer risk.

Modeling the dispersion of radioactive release and their subsequent environmental and health impact have been a topic of interest for several decades. To this end, numerous mathematical models have been developed to simulate the transport of radioactive materials in the atmosphere and their subsequent fallout on land and sea. The most preferred and recommended computer models are typically based on mathematical approaches such as Eulerian, Lagrangian, and Gaussian. The Gaussian approach is widely accepted and used by many organizations and countries. For example, the U.S. Environmental Protection Agency (U.S. EPA) has developed several codes using the Gaussian approach, such as AERMOD, CALPUFF, and CALINE3, among others. Germany has developed a Gaussian puff dispersion and deposition model called ATSTEP, which is used in the RODOS real-time decision support system for nuclear emergency management. The PUFF-PLUME Gaussian radionuclide dispersion model, developed by Pacific Northwest National Laboratory (PNNL), is currently the primary model used by the U. S. Department of Energy for emergency response. Many studies have utilized these mathematical approaches to analyse past nuclear accidents, such as Chernobyl and Fukushima. For instance, [9] applied a three-dimensional model to simulate radionuclides in the marine environment. Conceptually similar work has been conducted by [10], focusing on the migration behaviors of Cs-137 in different sediment layers. Several authors have recognized the Lagrangian particle dispersion model for estimating ground deposition [11-13]. [14] proposed a theoretical algorithm for modeling the dispersion of I-131 based on the Eulerian advection-diffusion equation. [15] utilized short- and long-term dispersion models based on the Gaussian distribution. These models have been applied not only to the past nuclear accidents but also to hypothetical nuclear reactor scenarios. For example, [16-17] studied the atmospheric dispersion and dose assessment of the most dangerous radionuclides from a hypothetical accident at an NPP in Southeast Asia on a local scale, using the Hybrid Single-Particle Lagrangian Integrated Trajectory Model, commonly known as HYSPLIT. A similar methodological approach was used in the study by [18], employing the Lagrangian particle dispersion model FLEXPART. [19] performed a statistical validation of the FLEXPART model used for decision support systems. The Gaussian approach has also been widely used to model atmospheric dispersion and land deposition, particularly in hypothetical accident scenarios. [20] simulated a hypothetical accident for the Ghana research reactor using the Gaussian plume model and calculated radiological doses with the health physics code called HotSpot. [21] utilized the Gaussian-based RASCAL code to describe the atmospheric dispersion of different radionuclides under various meteorological scenarios. In the study conducted by [22], the deposition of radionuclides was analyzed by comparing dry and wet depositions. [23] performed a comparative analysis of hypothetical accident scenarios with different emission levels for the VVER-1200 nuclear reactor type. [24] researched the main consequences and risks of a hypothetical accident at the ITU TRIGA Mark II research reactor by applying integrated simulation models and considering various atmospheric conditions.

Our research considerers a hypothetical nuclear accident at the planned Akkuyu NPP in the Republic of Turkiye. At a national level, several previous studies have examined potential accident at Akkuyu NPP. For example, [25] focused on assessing the marine environment in the event of a nuclear accident. Similar work by [26] utilized a combination of hydrodynamic and radiobiological models to determine the distribution of radionuclides in marine organisms in the event of an accident at Akkuyu NPP. [27] investigated the doses received by the population from a hypothetical accident in Turkiye, considering effects not only at the regional scale but also the potential for ground contamination at a global level, including European countries. Although these studies have made significant contributions to national research, there is still a need for a more precise understanding of the effects of radioactive contamination on the population, which is crusial for mitigating the consequences of a nuclear accident. The aims of

our study are twofold: firstly, we aim to calculate the potential radiation doses and ground contamination from a hypothetical severe accident at Akkuyu NPP, using a scenario similar to the Fukushima Daiichi NPP accident, which involved a reactor core meltdown. Secondly, we aim to evaluate the adequacy of the current PAZ and EPZ and the likelihood of needing to take protective actions outside these zones in the event of a nuclear emergency. To simulate the dispersion of radionuclides, we used the Gaussian plume model with realistic weather scenarios. Land contamination and radiation doses were calculated using the HotSpot computer code, which allows estimation up to 100 km from the release point. After analyzing the results obtained from HotSpot, we identified the main protective actions based on the dose criteria according to safety requirments and guidelines of the IAEA. Our study will discuss potential protective measures that must be considered during the emergency phase, thereby providing valuable support to decision-makers for the effective management of a nuclear accident, if one occurs.

Materials and Methodology

A flow diagram of the methodology adopted in the present study is shown in Figure 1, with details provided in subsequent sections. Our approach starts with identifying the amount of radioactive release during a potential accident scenario, considering the duration over which radionuclides may disperse and the potential release height. The atmospheric dispersion and transport of the radioactive release are simulated based on meteorological parameters such as wind speed, wind direction, and atmospheric stability class. Estimated values of air concentration and ground deposition are then used to calculate the expected doses that the accident may cause to the public through the passing plume. Finally, based on the calculated doses, the size of the EPZs is determined along with the corresponding protective measures.

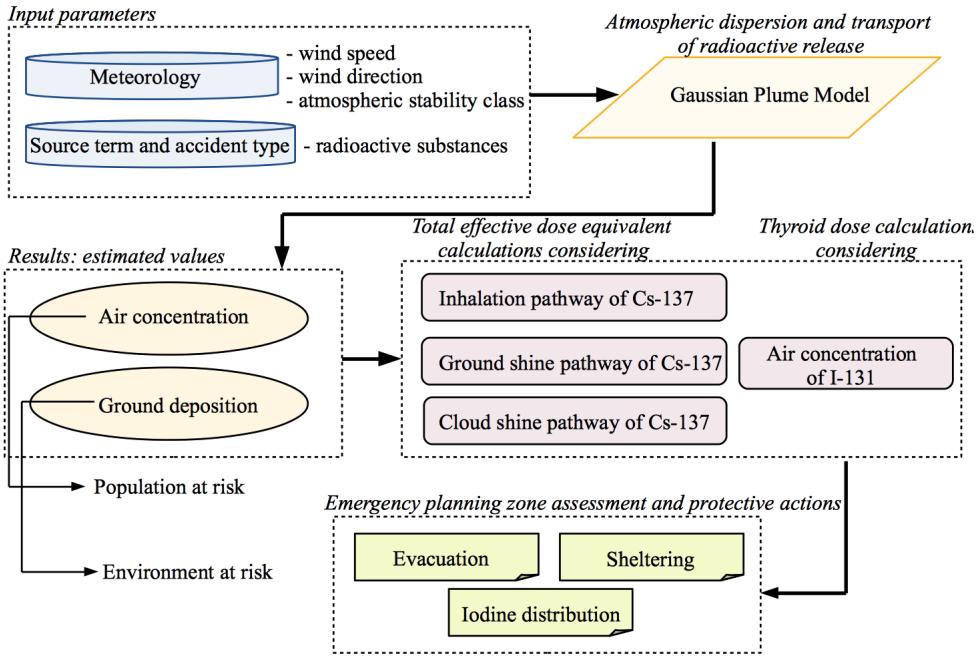

Figure 1. Workflow diagram for assessing emergency planning zones and determining appropriate protective measures

The first NPP in Turkiye: Site Location and the National Radiation Emergency Plan

Akkuyu NPP is the first nuclear power project in the Republic of Turkiye and is currently the largest nuclear facility under construction in the world [28]. It will be equipped with four power units featuring the latest VVER-1200 type reactors. The estimated operating life of the Akkuyu NPP is 60 years, with a possible extension for another 20 years. The Akkuyu NPP is expected to provide reliable energy supplies to nearly 10 million consumers in more than 10 provinces of the country [29-30].

Akkuyu NPP is geographically located in the Mersin province in the Mediterranean region in the southern part of Turkiye (Figure 2). The famous tourist center and densely populated city of Antalya is located west of the NPP site, approximately 300 km away, with a population over 2 million people. Other metropolitan areas such as Mersin and Adana (with population of 1,916,432 and 1,814,00, respectively, as of 2022) are located to the northeast of the site at distances of 140 and 217 km, respectively. The island of Cyprus is located nearly 100 km south of the plant in the Mediterranean Sea. Additionally, within the 100 km zone, there are 7 districts with a total population of 482,520 people. Figure 2 illustrates the population in each district along with the area. The most populated areas are located to the northeast of the NPP, while the western areas have the lowest population density.

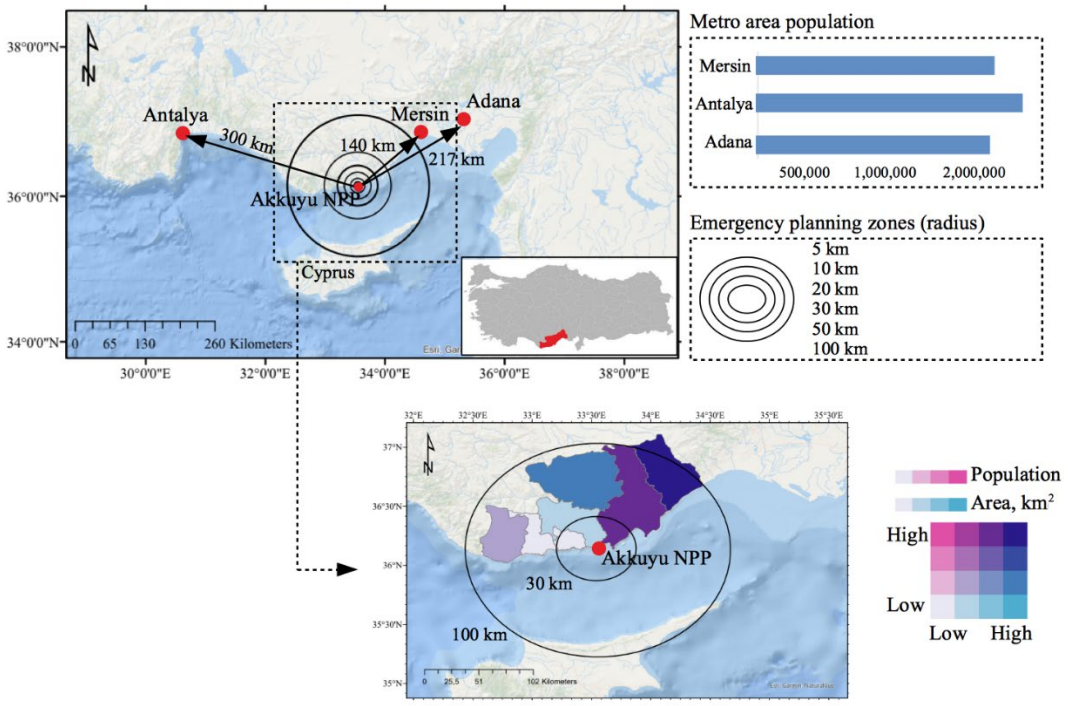

Figure 2. Akkuyu NPP site location and neighbouring areas

In 2019, two national organizations, the Nuclear Regulatory Authority (NRA) and the Disaster and Emergency Management Authority (DEMA), developed a National Radiation Emergency Plan (*Ulusal Radyolojik Acil Eylem Planı – URAP in Turkish*). According to this plan, EPZs are defined as having a 5 km radius for the PAZ, a 20 km radius for the UPZ, a 100 km radius for the EPD, and a 300 km radius for the ICPD (Figure 2) [31]. These boundaries were determined by considering geographical and topographical features to ensure that emergency responders can easily navigate the situation. However, since the consequences of an NPP accident primarily concern environmental and health issues, EPZs must also take into account Land Use Land Cover (LULC) classification and demographics [32].

Weather Data

Data describing the predominant atmospheric conditions, including wind speed and direction during a nuclear accident, are crusial for atmospheric dispersion models. Furthermore, the distribution of radioactive materials in the air and their subsequent deposition on land are highly dependent on both the prevailing wind conditions and atmospheric disturbances, which are influenced by the stability of the atmosphere. The most widely used method for classifying atmospheric stability is the Pasquill-Turner scheme, developed by Pasquill and modified by Turner [33]. According to this scheme, atmospheric stability is classified into six different classes: A, B, C, D, E, and F. Class-A describes the most unstable or turbulent conditions, while Class-F corresponds to the most stable or least turbulent conditions. In the present study, atmospheric radioisotope dispersion modeling and associated dose estimation were investigated for each of these atmospheric stability classes, as they are all relevant to the study area. Figure 3 shows wind speed variations in each direction according to atmospheric stability class for the current study area. It can be seen that wind speeds mostly fall within the range of 0.5 m/s to 3.6 m/s.

Although higher speeds are also observed in the study area, they are less frequent. Additionally, Mersin province experiences a fairly dry climate, with minimal rainfall throughout the year. The total annual rainfall is approximately 600 mm, with the highest rainfall occurring in winter and spread over about 15 days. For this reason, only the effects of dry deposition were investigated.

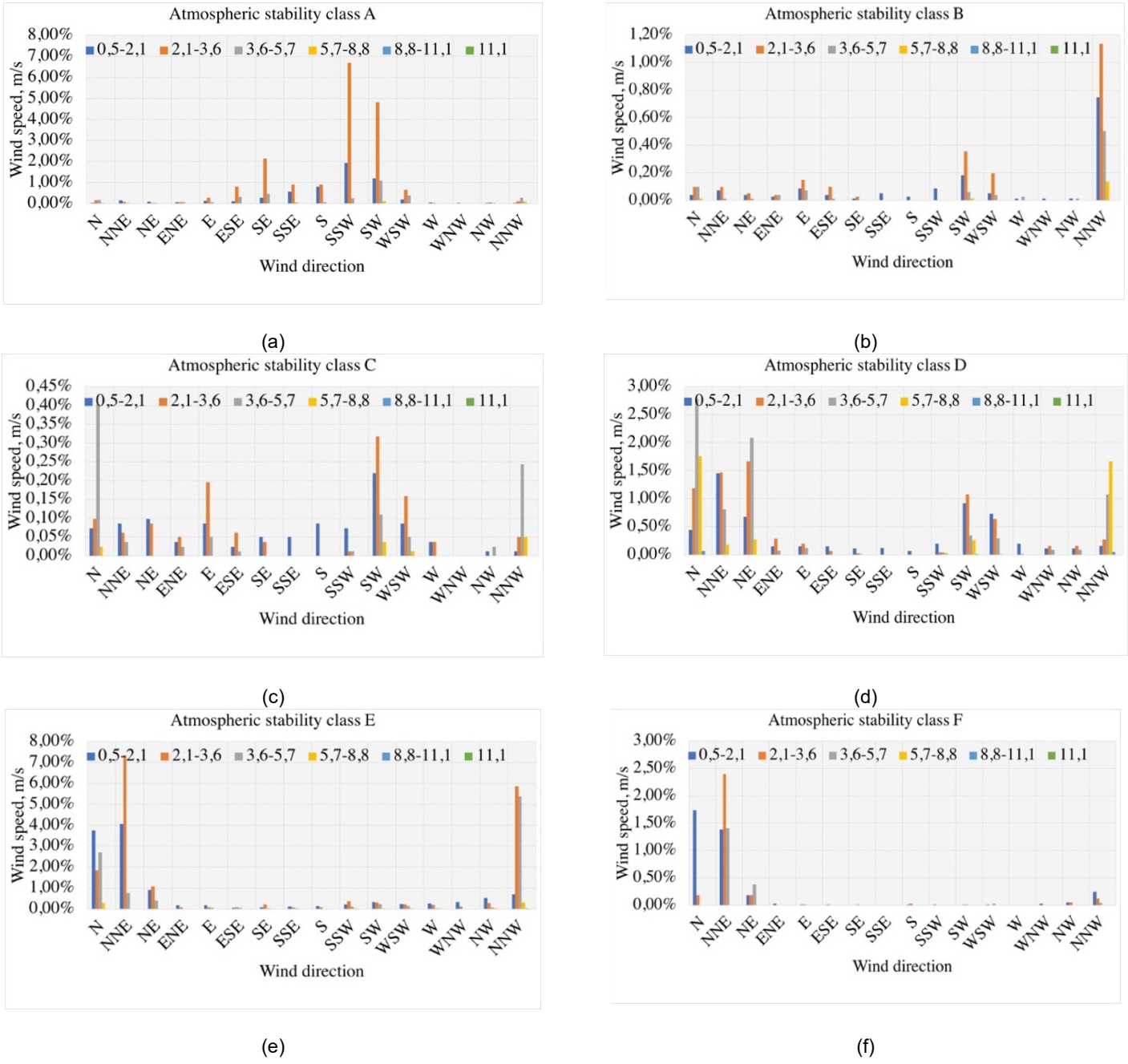

Figure 3. Wind speed frequency: (a) stability Class-A; (b) stability Class-B; (c) stability Class-C; (d) stability Class-D; (e) stability Class-E; (f) stability Class-F

Since the NPP is located at a coastal area, our study considered only those wind directions that predominantly affect populated areas, namely, from east (E) to west (W) in a clockwise direction. Table 1 lists the meteorological scenarios considered in the study. According to Table 1, the most frequently occurring stability classes are A, D, and F, with occurrences of 26.7%, 26.3%, and 30.5%, respectively.

Table 1. Meteorological data used for atmospheric dispersion simulations

Atmospheric stability class and frequency of its occurrence (%)		Wind directions and corresponding wind speed (m/s)								
		E	ESE	SE	SSE	S	SSW	SW	WSW	W
A	26.7	3.6	3.6	3.6	3.6	3.6	3.6	3.6	3.6	2.1
B	3.5	3.6	3.6	3.6	2.1	2.1	2.1	3.6	3.6	5.7
C	4.4	3.6	3.6	2.1	2.1	2.1	3.6	3.6	3.6	3.6
D	26.3	3.6	2.1	2.1	2.1	2.1	2.1	3.6	2.1	2.1
E	30.5	2.1	3.6	3.6	2.1	2.1	3.6	2.1	2.1	2.1
F	8.6	3.6	2.1	3.6	2.1	3.6	2.1	2.1	5.7	2.1

Accident Scenario and Source Term

In this study, a core meltdown accident was used because the radiological consequences are more severe than those of other types of accidents. It is assumed that the accident occured due to the failure of one of the four operating reactors. During such an accident, a variety of radioisotopes are released into the environment, including radionuclides of noble gases (Krypton, Xenon, Radon), halogens (Fluorine, Bromine, Iodine), alkali metals (Cesium, Rubidium, Lithium), cerium groups, and noble metals (Ruthenium, Rhodium, Iridium), among others. The quantity of released radionuclides, known as the source of radioactivity, depends on the NPP design and is usually estimated using computer codes [21, 23]. For radiation protection purposes, cesium (Cs-137) and iodine (I-131) are of particular importance due to their harmful radioactive properties. Cs-137 is particularly dangerous for the environment because it is absorbed by vegetation and poses a long-term exposure risk. Its physical half-life is 30 years, and its compounds can travel long distances through the air before settling on the ground [34]. Despite its relatively short half-life of 8 days, I-131 is a concern because it is absorbed by the thyroid gland upon consumption, exposing it to radiation and potentially increasing the risk of thyroid cancer. Therefore, this study focuses on the most important radioactive materials, namely Cs-137 and I-131. According to [35], these radionuclides dominate the source term, with more than 60% and 30% of the total release activity, respectively, while contributions from other groups are less than 10%. The Cs-137 and I-131 emissions used in this study are similar to those from the Fukushima accident and are approximately an order of magnitude lower than those from the Chernobyl accident. The Fukushima accident was reported to have released up to 20 PBq of Cs-137 and about 400 PBq of I-131, while the Chernobyl accident released about 2000 PBq and 90PBq of Cs-137 and I-131, respectively [36]. Therefore, in our study, the activity releases for Cs-137 and I-131 were selected to be 1.20×10^{17} Bq and 3.20×10^{18} Bq, respectively. The effective release height was chosen to be 100 m, and the duration of the accident was assumed to be 48 hours.

Modeling Dispersion and Deposition

One of the most widely used atmospheric dispersion models is the HotSpot code, developed to assist emergency responders by providing fast computations in the initial hours of an emergency situation [37]. HotSpot uses the Gaussian Plume Model, which calculates the likely air concentration of radionuclides downwind of a release point by defining several parameters: (1) atmospheric stability class; (2) wind speed at the release height; (3) plume rise; (4) dispersion parameters; and (5) radionuclide concentration.

The general equation of the Gaussian dispersion model assumes that the dispersion of radionuclides is normally distributed in directions perpendicular to the wind directions and can be expressed by formula (1).

$$C(x,y,z) = \left(\frac{Q}{U_s}\right)\left(\frac{1}{2\pi\sigma_x\sigma_y}\right) exp\left[-\frac{y^2}{2\sigma_y}\right]\left(exp\left[-\frac{(H_s-z)^2}{2\sigma_z^2}\right] + exp\left[-\frac{(H_s+z)^2}{2\sigma_z^2}\right]\right) \quad (1)$$

where C is a radionuclide concentration (Bq/m^3); Q is an emission rate (Bq/s); U_s corresponds to the wind speed at the release height (m/s); σ_y and σ_z are lateral and vertical dispersion parameters (m); y relates to the crosswind distance (m); z is an elevation of receiver (m); and H_s is a release height (m).

Effective Dose Calculations and Stochastic Health Effects

After an NPP accident, the population is exposed to radioactive materials in several ways: (1) external exposure from radionuclides deposited on the land (groundshine); (2) external exposure from radionuclides concentrated in the radioactive cloud (cloudshine); and (3) internal exposure from the intake of radionuclides [38]. These exposure pathways were considered in the assessment to calculate

the Total Effective Dose Equivalent (TEDE). TEDE is defined by the US Nuclear Regulatory Commission as a radiation dosimetry quantity used to monitor and control human exposure to radiation. In this study, TEDE values and thyroid doses were calculated using the HotSpot code for dose assessment. The calculation procedure is explained through a series of equations listed below.
Inhalation dose can be calculated using equation (2):

$$D_{inh} = C_A \times V_B \times DC_{inh} \times R_{inh} \quad (2)$$

where D_{inh} is an inhalation dose (Sv); C_A corresponds to the air concentration (Bq/m^3); V_B is a breathing rate (m^3/day); DC_{inh} relates to radionuclide specific dose conversion factor for inhalation (Sv/Bq); R_{inh} is a reduction factor.

The reduction factor, R_{inh}, can be calculated by the following equation (3):

$$R_{inh} = F_{in} \times C_{in} + F_{out} \times C_{out} \quad (3)$$

where F_{in} and F_{out} are fractions of time spent indoor and outdoor, respectively; C_{in} and C_{out} are indoor and outdoor reduction factors.

External cloud dose is calculated using the following relation (4):

$$D_{cloud} = C_a \times DCF_{cloud} \times R_{cloud} \quad (4)$$

where D_{cloud} is a cloudshine dose (Sv); C_a is the air concentration (Bq/m^3); DCF_{cloud} relates to a cloudshine dose conversion factor (Sv×m^3/Bq×s); and R_{cloud} corresponds to reduction factor which is calculated using the equation below (5):

$$R_{cloud} = \sum f_i \times c_j \quad (5)$$

where f_i –fraction of time staying at outdoor location i and c_j is a correction coefficient for the gamma dose rate at outdoor location i.

External ground dose is calculated using equation (6):

$$D_{ground}(T) = GC(t) \times R_{ground} \times DC_{ground} \times \exp(-\lambda) \quad (6)$$

where D_{ground} (T) relates to the groundshine dose (Sv) considering the time of fallout T; $GC(t)$ is the amount of deposition (Bq/m^2); R_{ground} is a reduction factor for staying indoors; DC_{ground} corresponds to the groundshine dose conversion factor (Sv×m^2/Bq×s); λ is a decay constant (1/day) and equal to 7.35E-10 and 9.98E-07 for Cs-137 and I-131, respectively.

TEDE doses are then calculated as the sum of the effective dose equivalent (for external exposure) and the committed effective dose equivalent (for internal exposures) using equation (7):

$$TEDE = D_{inh} + D_{cloud} + D_{ground} \quad (7)$$

Table 2 lists breathing rates and dose conversion factors used in equations (2), (4), and (6).

Table 2. Breathing rates and dose conversion factors [38]

Radionuclide	Breathing rate (m^3/day)	Cloudshine dose conversion factor (Sv.m^3/Bq.s)	Groundshine dose conversion factor (Sv.m^3/Bq.s)
Cs-137	22.2	3.89E-16	2.57E-19
I-131	22.2	1.69E-14	1.09E-17

In this study, stochastic health effects from Cs-137, including fatal and non-fatal cancer risks as well as severe hereditary health effects, were investigated. Individual stochastic risk can be calculated using equation (8).

$$R = TEDE \times R_{factor} \quad (8)$$

where TEDE relates to the dose calculated from equation (7); R_{factor} corresponds to the number of fatal cancers per million people for a single exposure of 10^{-2} Sv, considering the natural cancer incidence of the country's population. Table 3 lists the nominal probability coefficients for stochastic effects.

Table 3. Coefficients of stochastic effects (Sv^{-1})

Type of probabilistic effect	Fatal cancer	Non-fatal cancer	Severe hereditary effects
Value	5.0E-02	1.0E-02	1.3E-02

Results and Discussion

Ground deposition

During a nuclear emergency, assessing Cs-137 fallout following the passage of a radioactive cloud is crusial for evaluating levels of ground contamination and external exposure from radionuclides deposited on the land. This assessment is also important for further monitoring of food and water restrictions. The deposition of Cs-137 48 hours after the hypothetical radioactive release was calculated according to the stability classes and wind directions predominant towards populated areas. These numerical results are shown in Figure 4.

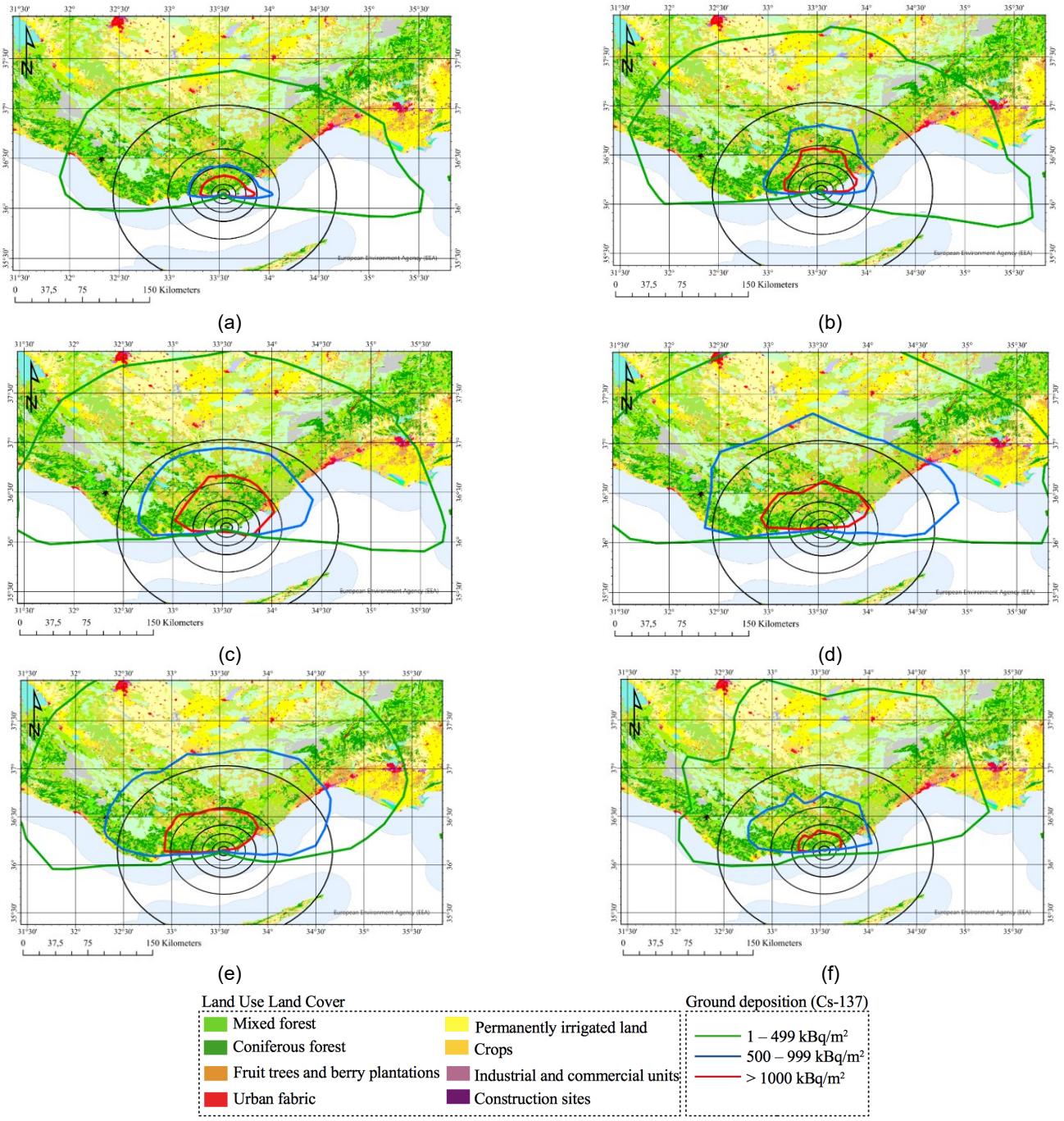

Figure 4. Spatial distribution of ground deposition values for Cs-137: (a) stability Class-A; (b) stability Class-B; (c) stability Class-C; (d) stability Class-D; (e) stability Class-E; (f) stability Class-F

Overall, as expected, the spatial distribution of activity deposition can vary depending on the meteorological stability class. Areas with Cs-137 levels higher than 1000 kBq/m^2 exceeded 50 km radius for C, D, and E stability classes. Regions with deposition values between 500 and 999 kBq/m^2 were found to extend beyond 100 km for D and E classes. Table 4 shows the total areas of ground deposition levels. Calculations of deposition indicate that a total area of nearly 4,000 km^2 will be exposed to the highest contamination level of more than 1000 KBq/m^2 during the Class-C, while the smallest area was calculated for Class-F. The medium risk zone has the highest contaminated area during Class-D and the lowest area in Class-A. From Figure 4, almost 80% of the entire Mersin province lies within the food sampling area boundaries, meaning that food production in this zone will be exposed to radiation in the event of a disaster. According to [39], the total area of agricultural land in Mersin is 406,000 hectares, with 65% used for dry agriculture and 35% for irrigated agriculture. A variety of plants are produced and cultivated, including wheat, banana, apricot, strawberry, and citrus. The share of vegetables, fruits and citrus, and livestock and animal production are 23%, 1.2%, and 44%, respectively. Moreover, lemons account for 34% of Turkiye's total citrus export. Additionally, as noted by [39], changes in land cover over recent years are expected to lead to an increase in fruit gardens as well as the expansion of human settlements, transport, and industrial areas. Therefore, it is necessary to recognize that all these resources may be at risk, and planning at various scales must be carried out correctly, considering the consequences of a hypothetical accident.

Table 4. Total area of Cs-137 ground contamination 48 hours after the hypothetical accident (km^2)

	Class-A	Class-B	Class-C	Class-D	Class-E	Class-F
High risk zone (>1000 kBq/m^2)	750	2,380	3,919	3,523	3,244	655
Medium risk zone 500–999 kBq/m^2)	1,868	5,728	11,812	22,900	20,480	5,712
Low risk zone (1–499 kBq/m^2)	39,163	57,201	66,553	76,413	70,453	46,071

Table 5 lists descriptive statistics of deposition values for each stability class. The highest ground deposition was calculated as 4.6E+05 kBq/m^2 for Class-C and 3.9E+05 kBq/m^2 for the Class-B at a distance of 1 km from the source. The minimum value of Cs-137 deposition was found to be 1.1E+02 kBq/m^2 for Class-A at a distance of 80 km from the accident site. The mean values of deposition within the PAZ were 7.4E+04 kBq/m^2, 1.4E+05 kBq/m^2, 2.1E+05 kBq/m^2, 3.2E+05 kBq/m^2, 1.4E+05 kBq/m^2, and 3.4E+04 kBq/m^2 for Classes-A, B, C, D, E, and F, respectively. The averages of Cs-137 deposited within the UPZ were 4.2E+03 kBq/m^2, 9.6E+03 kBq/m^2, 2.9E+04 kBq/m^2, 7.4E+04 kBq/m^2, 4.4E+04 kBq/m^2, and 9.7E+03 kBq/m^2 for Classes-A, B, C, D, E, and F, respectively.

Table 5. Statistics for Cs-137 ground contamination level (kBq/m^2)

Stability class	Maximum value	Mean value within PAZ	Mean value within UPZ
A	2.1E+05 at 1 km	7.4E+04	4.2E+03
B	3.9E+05 at 1 km	1.4E+05	9.6E+03
C	4.6E+05 at 1 km	2.1E+05	2.9E+04
D	7.9E+05 at 2 km	3.2E+05	7.4E+04
E	2.3E+05 at 2 km	1.4E+05	4.4E+04
F	5.0E+04 at 2 km	3.4E+04	9.7E+03

TEDE, Thyroid Doses, and Stochastic Health Effects

Since the goal of the research is to assess the potentially affected areas and establish protective actions, the TEDE areas were categorized into three classes: (1) high risk zone; (2) medium risk zone; and (3) low risk zone. The high-risk zone corresponds to the evacuation zone with radiation levels greater than 50 mSv, the medium risk zone corresponds to the sheltering zone with radiation levels between 10 mSv to 50 mSv, and the low-risk zone corresponds to areas with TEDE levels less than 10 mSv. Figure 5 depicts the TEDE and thyroid dosed of all six stability classes at various wind speeds. Doses were calculated for the first 48 hours after the accident up to a distance of 80 km from the NPP. As Classes-A and B are very unstable, the plume usually does not dissipate over longer distances. Therefore, the maximum distance for TEDE exceeding 50 mSv is 4 km, and for TEDE between 10 mSv and 50 mSv is 10 km during a wind speed of 2 m/s. For Classes-C, D and E, the plume spreads further with increasing activity levels compared to Classes-A and B. Thus, the evacuation distances reach 15 km, 40 km, and 35 km for Classes-C, D, and E, respectively, at a wind speed of 2 m/s. Figure 5 also shows that lower wind speeds allow for higher accumulation of TEDE values. For thyroid doses, doses exceeding 50 mSv reach 78-79 km from the release point for almost all stability classes, indicating the need for iodine distribution.

Consequently, as the downwind distance increases, TEDE decreases, with doses for Class-A being lower than those for the other classes. As atmospheric instability increases, the vertical dispersion of radioactive aerosols also increases, leading to lower concentrations deposited at specific locations. Radiation doses tend to rise steadily as the environment stabilizes, with maximum values observed in Classes D and E. It is notable that doses for Class-E are higher than those for Class-F. This anomaly can be attributed to the plume depletion effect, which causes concentrations to decline more rapidly with increasing stability class and deposition rate. Thus, the worst-case stability at longer downwind distances is not always associated with the highest stability. Because Class-E experiences less plume depletion than Class-F, it is possible for Class-E to produce higher local concentration than Class-F at a given location. Therefore, the more unstable the atmosphere, the more pronounced the dilution of radioactive aerosols; conversely, the more stable the atmosphere, the greater the radiation harm. Under normal weather conditions, TEDE clearly decreases as wind speed increases. Higher wind speeds are beneficial for minimizing radioactive hazards, as they transport radionuclides further downwind.

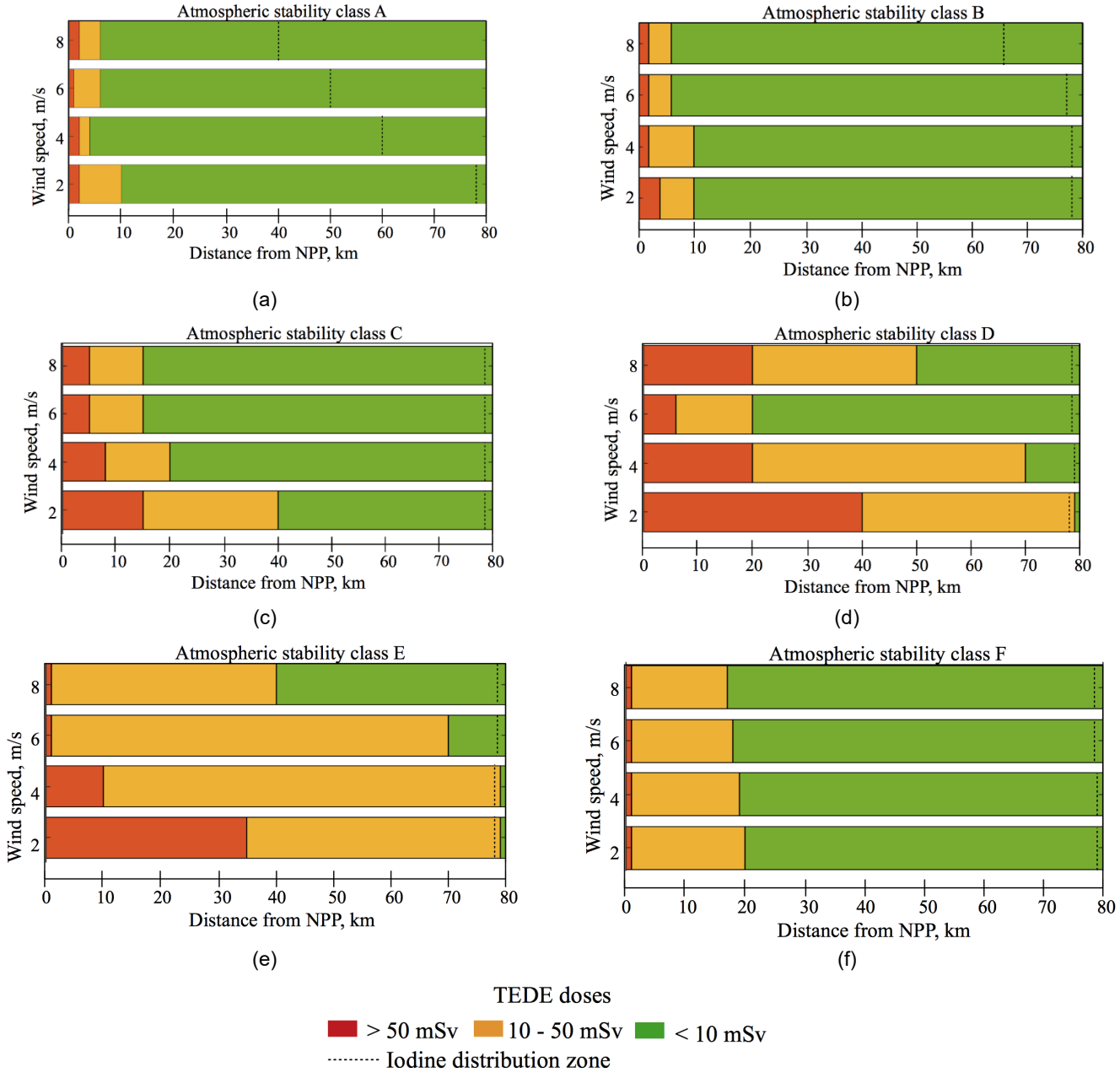

Figure 5. TEDE and thyroid doses calculated with accordance to the atmospheric stability classes

Figure 6 illustrates the collective health risk calculated for different stability classes within the 0-5 km, 5-10 km, 10-15 km, 15-20 km, 20-25 km, and 25-30 km radius zones. The greatest consequences of a potential accident at the Akkuyu NPP are expected for Classes-D and E. For example, within the 0-5 km radius zone for the Class-D, 52 people are predicted to develop fatal cancer, 10 people would likely suffer from non-fatal cancer, and 1 person would experience inherited effects of radiation. For Class-E, within the same zone, it is estimated that 26 people would develop fatal cancer, 5 would have non-fatal caner, and 1 person would suffer from genetic inheritance. For Classes-A and B, fatal cancer effects are estimated to affect 1 to 4 persons, with no non-fatal cancer effects observed under these meteorological conditions. Severe hereditary effects were not observed for Classes-A, B, C, and F, with a total of 6 and 5 persons affected in Classes-D and E, respectively. Table 6 lists the total number of people exposed to health risks within the 0-30 km radius zone. Therefore, approximately 45 and 35 fatal cancer cases per 10,000 people are expected under the meteorological conditions of Classes-D and E, respectively.

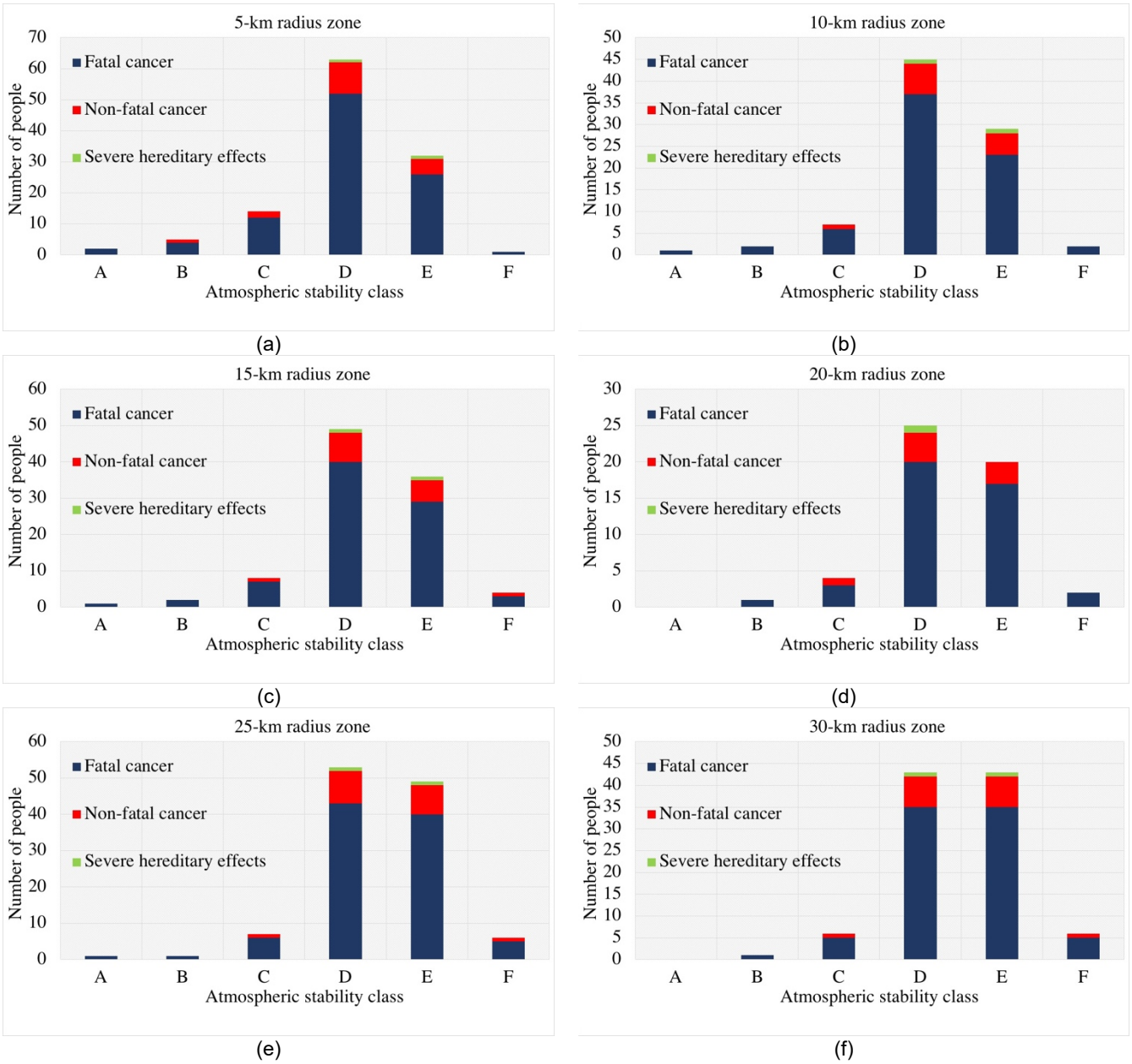

Figure 6. Collective health risk posed by the hypothetical accident: (a) 0-5 km radius zone; (b) 5-10 km radius zone; (c) 10-15 km radius zone; (d) 15-20 km radius zone; (e) 20-25 km radius zone; (f) 25-30 km radius zone

Table 6. Total number of people exposed to health risks within a 30-km radius zone

Collective health risk	Atmospheric stability class					
	A	B	C	D	E	F
Fatal cancer	5	11	39	227	170	18
Non-fatal cancer	0	1	7	45	34	3
Severe hereditary effects	0	0	0	6	5	0

Protective Actions

According to the IAEA, the main protective actions during a nuclear accident include evacuation, sheltering, and iodine prophylaxis [40]. Evacuation involves physically removing of population from an endangered area to a safer location, while sheltering-in-place means staying indoors to reduce exposure to outdoor hazard. Any building can serve as a shelter if it has a centrally located room or basement with as few windows or doors as possible. Iodine prophylaxis is carried out using iodine tablets to limit the effects of radiation and protect the body from radioactive I-131, thereby reducing the risk of thyroid cancer. Administrating iodine tablets is especially useful when I-131 is released into the atmosphere. Evacuation and sheltering measures are determined based on projected TEDEs, while iodine prophylaxis is recommended based on expected thyroid doses. Table 7 lists the threshold values for these protective measures according to guidelines established by various organization.

Table 7. Protective actions to be announced for the early phase of a nuclear emergency based on the projected radiation doses [40-42]

Protective action following the accident	Intervention levels for protective actions		
	IAEA*	U.S. EPA**	ICRP***
Evacuation	>50 mSv for TEDE	50 mSv for TEDE (expected exposure period of 4 days)	500 mSv for the whole body (averted dose)
Sheltering	10-50 mSv for TEDE	10 mSv for TEDE (expected exposure period of 4 days)	50 mSv (averted dose)
Iodine distribution	>50 mSv for thyroid dose	50 mSv for thyroid dose	50o mSv for thyroid dose (averted dose)

*IAEA – International Atomic Energy Agency
**U.S. EPA – United States Environmental Protection Agency
***ICRP – International Commission on Radiological Protection

In this study, TEDE and thyroid doses were calculated under the assumption that no protective measures, such as mandatory evacuation, sheltering in place, or iodine prophylaxis, were taken. We also assumed that the population remained outdoors during the entire duration of the radioactive plume passage. The results indicate that within the PAZ and UPZ, doses of both TEDE and thyroid radiation can significantly exceed the recommended limits. The suggested protective actions are listed in Table 8.

Table 8. Protective measures aimed at responding to a hypothetical accident at the Akkuyu NPP under various weather conditions

Stability class	TEDE and thyroid doses as a function of downwind distance (mSv)	Required protective actions
A	Up to 2 km when wind speed is 2 m/s, 4 m/s, and 6 m/s, TEDE > 50. Up to 1 km when wind speed is 8 m/s, TEDE > 50. Between 2 km and 10 km, 2 km and 4 km, 1 km and 6 km, 2 km and 6 km, when wind speed is 2 m/s, 4 m/s, 6 m/s, and 8 m/s, respectively, TEDE is in the range of 10-50. Thyroid doses are more than 50 up to 78 km, 60 km, 50 km, and 40 km during the wind speed of 2 m/s, 4 m/s, 6 m/s, and 8 m/s, respectively.	0-2 km: Evacuation 2-10 km: Sheltering 0-80 km: Iodine distribution
B	Up to 2 km when wind speed is 4 m/s, 6 m/s, and 8 m/s, TEDE > 50. Up to 4 km when wind speed is 2 m/s, TEDE > 50. Between 4 km and 10 km, 2 km and 10 km, 2 km and 6 km, 2 km and 6 km, when wind speed is 2 m/s, 4 m/s, 6 m/s, and 8 m/s, respectively, TEDE is in the range of 10-50. Thyroid doses are more than 50 up to 78 km, 78 km, 77 km, and 65 km during the wind speed of 2 m/s, 4 m/s, 6 m/s, and 8 m/s, respectively.	0-4 km: Evacuation 4-6 km: Sheltering 0-80 km: Iodine distribution
C	Up to 5 km when wind speed is 6 m/s and 8 m/s, TEDE > 50. Up to 8 km when wind speed is 4 m/s, TEDE > 50. Up to 15 km when wind speed is 2 m/s, TEDE > 50. Between 15 km and 40 km, 8 km and 20 km, 0 km and 5 km, 0 km and 6 km, when wind speed is 2 m/s, 4 m/s, 6 m/s, and 8 m/s, respectively, TEDE is in the range of 10-50. Thyroid doses are more than 50 up to 80 km during the wind speed of 2 m/s, 4 m/s, 6 m/s, and 8 m/s, respectively.	0-15 km: Evacuation 15-40 km: Sheltering 0-80 km: Iodine distribution
D	Up to 8 km when wind speed is 6 m/s, TEDE > 50. Up to 20 km when wind speed is 4 m/s and 8 m/s, TEDE > 50. Up to 40 km when wind speed is 2 m/s, TEDE > 50. Between 40 km and 79 km, 20 km and 70 km, 8 km and 20 km, 20 km and 50 km, when wind speed is 2 m/s, 4 m/s, 6 m/s, and 8 m/s, respectively, TEDE is in the range of 10-50. Thyroid doses are more than 50 up to 80 km during the wind speed of 2 m/s, 4 m/s, 6 m/s, and 8 m/s, respectively.	0-40 km: Evacuation 40-80 km: Sheltering 0-80 km: Iodine distribution
E	Up to 1 km when wind speed is 6 m/s and 8 m/s, TEDE > 50. Up to 10 km when wind speed is 4 m/s, TEDE > 50. Up to 35 km when wind speed is 2 m/s, TEDE > 50. Between 35 km and 79 km, 10 km and 79 km, 1 km and 70 km, 1 km and 40 km, when wind speed is 2 m/s, 4 m/s, 6 m/s, and 8 m/s, respectively, TEDE is in the range of 10-50. Thyroid doses are more than 50 up to 80 km during the wind speed of 2 m/s, 4 m/s, 6 m/s, and 8 m/s, respectively.	0-35 km: Evacuation 35-80 km: Sheltering 0-80 km: Iodine distribution
F	Up to 1 km when wind speed is 2 m/s, 4 m/s, 6 m/s and 8 m/s, TEDE > 50. Between 1 km and 20 km, 1 km and 19 km, 1 km and 18 km, 1 km and 17 km, when wind speed is 2 m/s, 4 m/s, 6 m/s, and 8 m/s, respectively, TEDE is in the range of 10-50. Thyroid doses are more than 50 up to 80 km during the wind speed of 2 m/s, 4 m/s, 6 m/s, and 8 m/s, respectively.	0-1 km: Evacuation 1-20 km: Sheltering 0-80 km: Iodine distribution

Conclusions

The aims of this work were to study the potential consequences of a hypothetical accident at the Akkuyu Nuclear Power Plant, the first nuclear reactor in Turkiye, and to assess the protective actions needed in case of such an accident. The potential consequences were estimated using a probabilistic approach for release under different meteorological conditions. In this study, we used a worst-case scenario with radionuclide release magnitudes similar to those of the Fukushima accident. Assessment was performed based on the deposition of Cs-137 on land, and TEDE and thyroid doses calculated from Cs-137 and I-131, each. Since Cs-137 and I-131 are considered the most harmful radioisotopes from environmental and health perspectives, we examined both in this study. The assessment was based on the IAEA dose criteria defined for protective actions. It was observed that the obtained dose rates and ground deposition maps correspond well to the wind conditions determined based on measurements from national weather station in the Akkuyu NPP area. This research suggest that the results are reliable and can be used for further studies of hypothetical accidents as well as for probabilistic risk assessments.

According to the results, it is unexpected that the dose criterion for evacuation outside the PAZ is exceeded during atmospheric stability classes such as A, B, and F. Hovewer, in the cases of Classes-C, D, and F, it is recommended to evacuate people outside the UPZ. Additionally, iodine prophylaxis is recommended up to a distance of 80 km, that is, outside the UPZ. For Classes A, B, and F, indoor sheltering is primary required within the UPZ, while for Classes C, D, and E, sheltering is needed for larger areas outside the UPZ. Due to the formation of Cs-137 deposits, temporary relocation of the population outside the 50-km radius zone may be required, along with limiting food and water consumption.

Acknowledgements

This paper is part of the PhD thesis of the first author conducted at Istanbul Technical University Graduate School. The weather data used in the dispersion modeling were provided by the Turkish State Meteorological Service. The demographic data were obtained from the Turkish Statistical Institute. The Land Use Land Cover maps were sourced from the Land Service of Copernicus, the Earth Observation Programme of the European Commission.

Conflict of Interest

The authors declare that they have no known competing financial interests or personal relationship that could face appeared to influence the work reported in this paper.

References

[1] Longmuir, C., & Agyapong, V. I. O. (2021). Social and mental health impact of nuclear disaster in survivors: A narrative review. *Behavioral Sciences, 11*(8), 113. https://doi.org/10.3390/bs11080113

[2] Takebayashi, Y., Lyamzina, Y., Suzuki, Y., & Murakami, M. (2017). Risk perception and anxiety regarding radiation after the 2011 Fukushima nuclear power plant accident: A systematic qualitative review. *International Journal of Environmental Research and Public Health, 14*(11), 1306. https://doi.org/10.3390/ijerph14111306

[3] Cléro, E., Ostroumova, E., Demoury, C., & others. (2021). Lessons learned from Chernobyl and Fukushima on thyroid cancer screening and recommendations in case of a future nuclear accident. *Environment International, 146*, 106230. https://doi.org/10.1016/j.envint.2020.106230

[4] Akiba, S. (2012). Epidemiological studies of Fukushima residents exposed to ionizing radiation from the Fukushima Daiichi Nuclear Power Plant prefecture: A preliminary review of current plans. *Journal of Radiological Protection, 32*(1), 1–10. https://doi.org/10.1088/0952-4746/32/1/1

[5] Batur, M., & Alkan, R. M. (2023). What can we learn from past nuclear accidents? A comparative assessment of emergency response to accidents at the Three Mile Island, Chernobyl, and Fukushima Nuclear Power Plants. *Advanced Land Management, 3*(2), 76–89.

[6] Saindane, S. S., Murali, S., Dhole, S. D., & Karmalkar, N. K. (2021). Planning, preparedness, and response to nuclear/radiological emergency. *Radiation Protection and Environment, 44*(1), 47–53. https://doi.org/10.4103/rpe.rpe_9_21

[7] Handl, G. (2016). Nuclear off-site emergency preparedness and response: Some international legal aspects. In J. Black-Branch & D. Fleck (Eds.), *Nuclear non-proliferation in International Law-Volume III* (pp. 229–245). T M C Asser Press. https://doi.org/10.1007/978-94-6265-138-8_11

[8] Dadda, A., Bouali, B., Bouam, A., Dahia, A., & Cheridi, A. L. D. (2024). Source term analysis and impact study during a hypothetical accident in Haiyang nuclear power plant. *Radiation Physics and Chemistry, 111542*. https://doi.org/10.1016/j.radphyschem.2024.111542

[9] Bacchi, V., & Tassi, P. (2019). Three-dimensional modeling of radionuclides dispersion in a marine environment with application to the Fukushima Dai-ichi case. *Environmental Modeling & Assessment, 24*, 457–477. https://doi.org/10.1007/s10666-018-9614-6

[10] Kumar, A., Rout, S., Chopra, M. K., & others. (2011). Modeling of Cs-137 migration in cores of marine sediments of Mumbai Harbor Bay. *Journal of Radioanalytical and Nuclear Chemistry, 301*, 615–626. https://doi.org/10.1007/s10967-014-3116-z

[11] Yasunari, T. J., Stohl, A., Hayano, R. S., Burkhart, J. F., Eckhardt, S., & Yasunari, T. (2011). Cesium-137 deposition and contamination of Japanese soils due to the Fukushima nuclear accident. *Proceedings of the National Academy of Sciences, 108*(49), 19530–19534. https://doi.org/10.1073/pnas.1112058108

[12] Chai, T., Draxler, R., & Stein, A. (2015). Source term estimation using air concentration measurements and a Lagrangian dispersion model: Experiments with pseudo and real cesium-137 observations from the Fukushima nuclear accident. *Atmospheric Environment, 106*, 241–251. https://doi.org/10.1016/j.atmosenv.2015.01.070

[13] Kovalets, I. V., Talerko, M., Synkevych, R., & Koval, S. (2022). Estimation of Cs-137 emissions during wildfires and dust storm in Chernobyl Exclusion Zone in April 2020 using ensemble iterative source inversion method. *Atmospheric Environment, 288*, 119305. https://doi.org/10.1016/j.atmosenv.2022.119305

[14] Tang, Z., Cai, J., Li, Q., & Zhao, J. (2019). The regional scale atmospheric dispersion of radionuclide I-131: A simulation method based on WRF-Chem model. *Radiation Physics and Chemistry, 156*, 81–93. https://doi.org/10.1016/j.radphyschem.2018.10.029

[15] Leelőssy, Á., Mészáros, R., & Lagzi, I. (2011). Short and long term dispersion patterns of radionuclides in the atmosphere around the Fukushima Nuclear Power Plant. *Journal of Environmental Radioactivity, 102*(12), 1117–1121. https://doi.org/10.1016/j.jenvrad.2011.07.010

[16] Muhamad, L. H., Karim, M. A., Chew, M. T., Kechik, M. M. A., Shah, N. M., Ibahim, M. J., & Saeed, I. M. (2023). Atmospheric dispersion and dose assessment of Cs-137 and I-131 from hypothetical incidents of nuclear power plant in Southeast Asia. *Radiation Physics and Chemistry, 208*, 110941. https://doi.org/10.1016/j.radphyschem.2023.110941

[17] Omar, N., Koh, M. H., & Hashmin, S. (2019). Radiological dose assessment due to hypothetical nuclear power plant operation in Mersing, Johor, Malaysia. *Malaysian Journal of Fundamental and Applied Sciences, 15*(4), 532–536. https://doi.org/10.11113/mjfas.v15n4.1397

[18] ElShafeey, N., Eid, M. M., Mahmoud, A. S., & Zakey, A. S. (2023). Risk assessment of possible hazards of El Dabaa Nuclear Power Plant using FLEXPART model. *Engineering Proceedings, 31*(1), 86. https://doi.org/10.3390/ASEC2022-13964

[19] Rakesh, P. T., Reddy, B. R., Srinivas, C. V., Shekhar, S. R., Venkatesan, R., Gopalakrishnan, V., & Venkatraman, B. (2021). Validation of a modified FLEXPART model for short-range radiological dispersion and dose assessments in ONERS decision support system. *Progress in Nuclear Energy, 136*, 103739. https://doi.org/10.1016/j.pnucene.2021.103739

[20] Birikorang, S. A., Abrefah, R. G., Sogbadji, R. B. M., Nyarko, B. J. B., Fletcher, J. J., & Akaho, E. H. K. (2015). Ground deposition assessment of radionuclides following a hypothetical release from Ghana Research Reactor-1 (GHARR-1) using atmospheric dispersion model. *Progress in Nuclear Energy, 79*, 96–103. https://doi.org/10.1016/j.pnucene.2014.11.013

[21] Ahangari, R., & Noori-Kalkhoran, O. (2019). A study of the protective actions for a hypothetical accident of the Bushehr nuclear power plant at different meteorological conditions. *Radiation and Environmental Biophysics, 58*, 277–285. https://doi.org/10.1007/s00411-018-00775-w

[22] Oboo, M., & Kim, J. (2024). Radiological consequence assessment from long term station blackout nuclear accident on Buyende nuclear power plant of Uganda. *Annals of Nuclear Energy, 199*, 110366. https://doi.org/10.1016/j.anucene.2024.110366

[23] Shiuli, S. S., Khaer, M. A., Islam, M. M., & others. (2022). Assessment of radiological safety and emergency response of VVER-1200 type reactor. *International Journal of Advanced Nuclear Reactor Design and Technology, 4*(2), 70–79. https://doi.org/10.1016/j.jandt.2022.04.002

[24] Bektaş, S., & Lüle, S. Ş. (2022). An integrated method for atmospheric dispersion and corresponding risks: Application to ITU TRIGA Mark II research reactor. *Progress in Nuclear Energy, 143*, 104039. https://doi.org/10.1016/j.pnucene.2021.104039

[25] Tsabaris, C., Eleftheriou, G., Tsiaras, K., & Triantafyllou, G. (2022). Distribution of dissolved Cs-137, I-131, and Pu-238 at eastern Mediterranean Sea in case of hypothetical accident at the Akkuyu nuclear power plant. *Journal of Environmental Radioactivity, 251*, 106964. https://doi.org/10.1016/j.jenvrad.2022.106964

[26] Abbasi, A., Zakaly, H. M., & Almousa, N. (2023). Radiotoxic fission products and radiological effects in the Mediterranean Sea biota from a hypothetical accident in Akkuyu Nuclear Power Plant. *Marine Pollution Bulletin, 193*, 115166. https://doi.org/10.1016/j.marpolbul.2023.115166

[27] Bilgic, E., & Gunduz, O. (2020). Dose and risk estimation of Cs-137 and I-131 released from a hypothetical accident in Akkuyu Nuclear Power Plant. *Journal of Environmental Radioactivity, 211*, 106082. https://doi.org/10.1016/j.jenvrad.2019.106082

[28] Agbulut, U., Ceylan, I., Gurel, A. E., & Ergun, A. (2021). The history of greenhouse gas emissions and relation with the nuclear energy policy for Turkey. *International Journal of Ambient Energy, 42*(12), 1447–1455. https://doi.org/10.1080/01430750.2018.1563818

[29] Aydın, C. I. (2020). Nuclear energy debate in Turkey: Stakeholders, policy alternatives, and governance issues. *Energy Policy, 136*, 111041. https://doi.org/10.1016/j.enpol.2019.111041

[30] Akar, A. U., Uyan, M., & Yalpir, S. (2023). Spatial evaluation of the nuclear power plant installation based on energy demand for sustainable energy policy. *Environment, Development and Sustainability*, 1–36. https://doi.org/10.1007/s10668-023-03061-y

[31] Turkish Ministry of Interior Disaster and Emergency Management Presidency. (2019). *Ulusal Radyasyon Acil Durum Plani (URAP)*.

[32] Iban, M. C., & Sahin, E. (2022). Monitoring land use and land cover change near a nuclear power plant

construction site: Akkuyu case, Turkey. *Environmental Monitoring and Assessment, 194*(10), 724. https://doi.org/10.1007/s10661-022-10437-6

[33] Hu, T., & Yoshie, R. (2020). Effect of atmospheric stability on air pollutant concentration and its generalization for real and idealized urban block models based on field observation data and wind tunnel experiments. *Journal of Wind Engineering and Industrial Aerodynamics, 207*, 104380. https://doi.org/10.1016/j.jweia.2020.104380

[34] Mensah, A. D., Terasaki, A., Aung, H. P., Toda, H., Suzuki, S., Tanaka, H., Onwona-Agyeman, S., Omari, R. A., & Bellingrath-Kimura, S. D. (2020). Influence of soil characteristics and land use type on existing fractions of radioactive Cs-137 in Fukushima soils. *Environments, 7*(2), 16. https://doi.org/10.3390/environments7020016

[35] Fairuz, A., & Sahadath, M. H. (2020). Assessment of the potential total effective dose (TED) and ground deposition (GD) following a hypothetical accident at the proposed Rooppur Nuclear Power Plant. *Applied Radiation and Isotopes, 158*, 109043. https://doi.org/10.1016/j.apradiso.2020.109043

[36] International Atomic Energy Agency (IAEA). (2015). *The Fukushima Daiichi Accident. Report by the Director General*. IAEA.

[37] Malizia, A., Chierici, A., Biancotto, S., & others. (2021). The HOTSPOT code as a tool to improve risk analysis during emergencies: Predicting I-131 and Cs-137 dispersion in the Fukushima nuclear accident. *International Journal of Safety and Security Engineering, 11*(4), 437–486. https://doi.org/10.18280/ijsse.110421

[38] Bellamy, M. B., Dewji, S. A., Leggett, R. W., & others. (2019). External exposure to radionuclides in air, water, and soil. *Federal Guidance Report, 15*, 402.

[39] Sandal, E. K., Adiguzel, F., & Karademir, N. (2020). Changes in land use between the years of 1990–2018 in Mersin province based on CORINE (Coordination of Information on the Environment) system. *Kastamonu University Journal of Engineering and Sciences, 6*(1), 8–18.

[40] International Atomic Energy Agency (IAEA). (2011). *Criteria for use in preparedness and response for a nuclear or radiological emergency: General safety guide*. IAEA Safety Standards Series No. GSG-2.

[41] International Commission on Radiological Protection (ICRP). (1992). *Principles for intervention for protection of the public in a radiological emergency* (ICRP Publication 63).

[42] U.S. Environmental Protection Agency (EPA). (2017). *Protective action guides and planning guidance for radiological incidents*. Radiation Protection Division.